PAPR reduction in PAM-DMT based WDM VLC

Alrakah, Hussien T.; Gutema, Tilahun Z.; Sinanovic, Sinan; Popoola, Wasiu O.

Published in:
2022 13th International Symposium on Communication Systems, Networks and Digital Signal Processing (CSNDSP)

DOI:
10.1109/CSNDSP54353.2022.9907952

Publication date:
2022

Document Version
Author accepted manuscript

PAPR Reduction in PAM-DMT based WDM VLC

Hussien T. Alrakah*†, Tilahun Z. Gutema*, Sinan Sinanovic‡, Wasiu O. Popoola*
*Institute for Digital Communications, School of Engineering.
The University of Edinburgh, Edinburgh, EH9 3FD, UK.
†Faculty of Computer Science and Information Technology.
Jazan University, Jazan, Kingdom of Saudi Arabia.
‡School of Engineering and Built Environment.
Glasgow Caledonian University, Glasgow, Scotland, UK.
h.alrakah@ed.ac.uk, tilahun.gutema@ed.ac.uk, sinan.sinanovic@gcu.ac.uk, w.popoola@ed.ac.uk

***Abstract*—Visible light communication (VLC) can achieve high data rate transmission with discrete multitone (DMT) systems. A DMT variant is pulse-amplitude-modulated discrete multitone modulation (PAM-DMT) which offers an energy-efficient modulation solution for VLC. However, similar to other DMT modulation techniques, PAM-DMT suffers from a high peak-to-average power ratio (PAPR). In this paper, the efficacy of pilot-assisted (PA) PAPR reduction system in PAM-DMT based VLC is demonstrated experimentally. Wavelength division multiplexing (WDM) is applied using three low-cost light emitting diodes (LEDs). The available modulation bandwidth of each light source is utilised by adaptive bit and power loading. PA PAM-DMT is compared in this work to PAM-DMT based on achievable data rate and Bit Error Rate (BER). The proposed system reduces the clipping noise and minimises the nonlinear distortion of the system by reducing the high PAPR of each wavelength. Thus, the PA PAM-DMT has achieved 8% higher data rate than the conventional PAM-DMT with no PAPR reduction.**

***Index Terms*—optical OFDM, optical wireless communication, visible light communication, Pulse-amplitude-modulated discrete multitone modulation PAM-DMT, peak-to-average power ratio PAPR, pilot-assisted PA, wavelength division multiplexing WDM.**

I. Introduction

In wireless communications (WC), there is continued interest in using the huge and unlicensed visible light communication (VLC) spectrum for high data rate transmission. VLC systems use low-cost commercially available off-the-shelf front end devices i.e. light emitting diodes (LEDs) and photodiodes (PDs). Furthermore, significant energy and cost saving can be enabled by reusing the existing lighting infrastructures [1]. The intensity modulation with direct detection (IM/DD) transmission mechanism in VLC restricts the transmitted signal to be real and positive [2]. Discrete multitone (DMT) modulation techniques are attractive candidates for VLC systems due to their multi-path propagation resilience, intersymbol interference (ISI) mitigation, and the simplified single-tap equalisation process [3].

Different DMT modulation variants have been proposed in order to enable modulation techniques for the IM/DD systems. In direct current (DC) optical orthogonal frequency division multiplexing (DCO-OFDM), the bipolar signal is converted to an unipolar by adding DC bias [4]. DCO-OFDM is energy inefficient due to DC bias that is required to make the signal unipolar [4]. Another option is asymmetrically clipped optical OFDM (ACO-OFDM) where the properties of Fourier transformation is used to load the information symbols on the odd-indexed subcarriers only while even subcarriers set to zeros. This results in an asymmetric property which allows the signal clipping at the zero level in the time domain without clipping distortion of the information symbols. This solution comes at the cost of spectral efficiency reduction by half [5]. To improve the spectral and energy inefficiency of ACO-OFDM and DCO-OFDM respectively, pulse-amplitude-modulated DMT (PAM-DMT) was proposed in [6]. In PAM-DMT, the PAM symbols are modulated onto the imaginary components while, the real parts are set to zeros. PAM-DMT activates all subcarriers and allows for asymmetrical clipping at zero level then transmit the imaginary positive samples of the DMT only. The clipping distortion falls on the real components [6].

Despite the advantages of DMT techniques, they are affected by high peak-to-average power ratio (PAPR). PAM-DMT is considered in this study where the bipolar signal is clipped at zero level to obtain the real time domain signal. Due to the limited dynamic range of VLC light sources and high PAPR of PAM-DMT system, the pilot-assisted (PA) scheme is applied to reduce the high PAPR values [3]. The PA PAPR reduction gain in PAM-DMT is presented in [7]. PAPR reduction minimises the clipping noise and the nonlinearity distortion introduced by the optical source.

In this paper, experimental demonstration of PA PAM-DMT based VLC using low-cost of-the-shelf LEDs is presented. The high PAPR values of PAM-DMT is reduced with PA scheme. Wavelength division multiplexing (WDM) system is utilised to efficiently modulate three different wavelengths in the VLC spectrum. Each channel bandwidth is utilised using adaptive bit and power loading. The PA PAM-DMT data rate per wavelength is evaluated and compared to that of conventional PAM-DMT without PAPR reduction.

The rest of this paper is organized as follows: Section II presents the optical PAM-DMT system description, the principle of PAPR reduction technique and bit-power loading. Experimental setup is presented in Section III, while the data transmission results and discussions are in Section IV. The paper is concluded in Section V.

II. System Description and Principle

A. Optical PAM-DMT

PAM-DMT system modulates the imaginary components of the complex-valued PAM symbols and, the real parts are set to zeros. This results in $X[k] = \jmath B_{\mathrm{PAM}}[k]$, where $B_{\mathrm{PAM}}[k]$ is the M-PAM symbols carrying useful data that are loaded on the imaginary components and k is the subcarrier index, where $k = 1, 2, \ldots, N/2-1$ and $N = 2(N_{\mathrm{subs}}+1)$ and N_{subs} is the active subcarriers carrying information [6]. PAM-DMT must satisfy the requirement of intensity modulation (IM) by generating real and non-negative LED modulating signal. The real-valued baseband waveform is achieved by imposing a Hermitian symmetry on the PAM symbols in the frequency domain. This is given by: $X[k] = X^*[N/2-k]$, where X^* indicates the conjugate of X and $X[0] = X[N/2] = 0$.

The time domain signal is obtained by applying inverse fast Fourier transform (IFFT) of size N to the frequency domain waveform which is given as the follows [6]:

$$x(n) = \frac{-2}{\sqrt{N}} \sum_{k=0}^{\frac{N}{2}-1} B_{\mathrm{PAM}}[k] \sin\left(2\pi n \frac{k}{N}\right) \tag{1}$$

where $(n = 0, 1, \ldots, N-1)$. The non-negative signal is obtained by clipping the negative part of PAM-DMT waveform at zero level. The time domain waveform of PAM-DMT follows an antisymmetry property and as a result, clipping the negative samples of $x(n)$ is distortion-less as the clipping distortions are transformed into the real domain of the subcarriers. The useful information can be recovered from the imaginary components at the receiver side [6], [8].

B. High PAPR Reduction with Pilot Assisted Technique

PAM-DMT allows asymmetric clipping at zero level and convey the useful information on the positive parts of the DMT signal $x(n)$ which makes the system power efficient by reducing the DC bias requirement to the minimum. However, the inherent high PAPR values of the system must be reduced to benefit from the full dynamic range of the optical source. The high PAPR will make the light source operates outside its linear dynamic region and causes upper level clipping by the frond-end devices of the system which introduce clipping noise and distortion to the transmitted signal [9].

To address the PAPR problem, the pilot assisted (PA) will be used to reduce the high PAPR of the PAM-DMT system. PA was proposed in [3], to rotate the phase of the DMT signal. However, its extension to PAM-DMT modulation technique is not straightforward. PA technique implementation for PAM-DMT system is described for VLC system in this section.

The electrical PAPR of the time domain PAM-DMT frames block is defined as follows [3]:

$$\mathrm{PAPR} = \frac{\max\limits_{0 \le n \le N-1} (|x(n)|^2)}{E[|x(n)|^2]} \tag{2}$$

where $\mathrm{E}[\cdot]$ is the statistical expectation. Complementary cumulative distribution function diagram (CCDF) is used to evaluate the PAPR as the most used measure for PAPR reduction [3]. The CCDF is defined as the probability that the PAM-DMT frames block PAPR exceeds a predefined reference value. High PAPR peaks appear when individual subcarriers added up coherently in time domain [10].

The procedure of using PA for PAPR reduction in PAM-DMT is described as follows [3]:

- Group PAM-DMT frames to U blocks comprise of active subcarriers N_{subs} in the frequency domain; where, $X^u[k]$, $u = 1, 2, \ldots, U$.
- Generate R different iterations of pilot candidates X_p^r, where $r = 1, 2, \ldots, R$.
- Set the amplitude of X_p^r sequence to ± 1.
- The phase $\theta_p(k)$ of the pilot sequence is randomly generated with only 0 or π values, $k = 1, 2, \ldots, N_{\mathrm{subs}}$.
- Calculate PAPR_r value of each pilot iteration of X_p^r.
- Select the pilot sequence $X_p = X_p^{\tilde{r}}$ that gives the minimum PAPR value for the transmission; where [9],

$$\tilde{r} = \arg \min_{1 \le r \le R} (\mathrm{PAPR}_r) \tag{3}$$

- Embedded the pilot sequence X_p into the corresponding PAM-DMT frames block U to reduce its PAPR, and as a result the number of frame per block will be $\hat{U} = (U+1)$, details can be found in [3].

In this work, number of PAM-DMT frames are grouped to form a block U, and $U = 5$ frames per block because the PAPR increases as U increases [3]. The number of iterations are selected to be $R = 10$ iterations as it shows a good trade off between performance and complexity [11]. Cyclic prefix (CP) is often not used when evaluating the PAPR of the system as it has negligible effect on the PAPR values. At the receiver side, the PA sequences are estimated using the maximum likelihood (ML) technique. The recovered PA phase is used to recover the phase of the corresponding block U of the received data prior to the equalization process [3].

C. Optical PAM-DMT with Adaptive Bit and Power Loading

VLC system has frequency-selective channel response which is attributed to the front-end devices frequency-dependent response and the optical channel itself [12]. PAM-DMT conveys the useful information on the positive imaginary components of the DMT signal activating all subcarriers of the system. Therefore, the PAM constellation format can be allocated adaptively at each subcarrier k to maximise the achievable data rate at a target bit error rate (BER). Thus, the VLC channel response and SNR per subcarrier SNR_k are estimated to allocate a suitable PAM constellation size to each subcarrier k based on the Levin-Campello algorithm [13]. This allows for higher modulation formats to be used for the subcarriers with higher SNR while ensuring that, the error probability P_e^T, is kept below the forward error correction (FEC) target of 3.8×10^{-3} [12]. In addition, the algorithm allows more power to be allocated to the subcarriers that require additional minimal energy to be elevated into higher constellation size while preserving the P_e^T. The adaptive

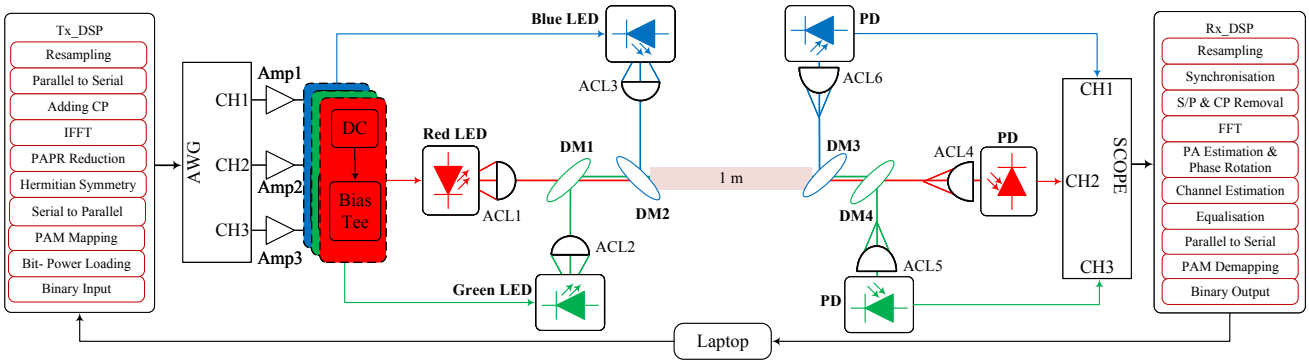

Fig. 1: Experimental setup block diagram

bit and power loading based on [13], can be formulated to optimise the following problems on each active subcarrier k [14]:

$$\text{maximise} \quad m_k = \log_2 M_k \tag{4a}$$

$$\text{subject to} \quad \text{BER}(M_k,\ \text{SNR}_k) \leq P_e^T \tag{4b}$$

$$\sum_{k=1}^{\frac{N}{2}-1} \nu_k^2 = N_{\text{subs}} \tag{4c}$$

where m_k is the number of bits per symbol with $m_k > 2$ bits and ν_k^2 is the power loading factor. $\text{BER}(\text{M}_k,\ \text{SNR}_k)$ is the theoretical BER equation of M_k-PAM at subcarrier k at corresponding SNR_k and can be approximated by the following [8]:

$$\text{BER}\left(M_k, \text{SNR}_k\right) \approx \frac{2}{\log_2 M_k} \times \left(1 - \frac{1}{M_k}\right) \times \sum_{l=1}^{\min(2,\sqrt{M_k})} Q\left((2l-1)\sqrt{\frac{6 \times \text{SNR}_k}{M_k^2 - 1}}\right) \tag{5}$$

where $Q(\cdot)$ is Gaussian Q-function. The overall data rate (R_b) of the bit and power loaded system can be calculated by [12]:

$$R_b = \frac{\sum_{k=1}^{\frac{N}{2}-1} \log_2 M_k}{(N + N_{\text{CP}})/2B} \tag{6}$$

where B is the single-sided modulation bandwidth of the system, and N_{CP} is the cyclic prefix size.

III. Experimental Setup

In this section, details of the experimental setup are presented. The WDM system uses three single colour LEDs for PAM-DMT with PAPR reduction transmission (PA PAM-DMT). The WDM LEDs are selected from Dialight with three different colours namely, red (R), green (G) and blue (B). The module numbers of RGB LEDs are Red: 598-8D10-107F - with wavelength of 635 nm, Green: 598-8081-107F with wavelength of 525 nm and Blue: 598-8D90-107F with 470 nm wavelength respectively [15]. The RGB single colour beams are combined at the transmitter (Tx) and separated at the receiver side (Rx) using two different Thorlabs dichroic mirrors on each side as shown in the system block diagram in Fig. 1.

The experimental setup starts with a laptop connected to an arbitrary waveform generator (AWG) (Keysight M8195A). The AWG has a sampling rate of 16 GSa/s and digital-to-analogue converter (DAC) resolution of 8 bits. The PA PAM-DMT waveforms with adaptive bit and power loading for each wavelength colour are generated in MATLAB as detailed in section (II) and, then transmitted to the AWG. The output of the AWG for each colour is amplified using (Mini-Circuits ZHL-1A-S+). Each amplified signal is then fed into a Bias-Tee (Mini-Circuits ZFBT-4R2GW) which combines the PA PAM-DMT information signal with the DC bias that comes from a DC power supply. The output of each Bias-Tee is connected to the corresponding LED. Since the half-power semi-angles of the selected LEDs are wide (i.e. 70°), aspheric condenser lenses (ACL1-3: Thorlabs ACL50832U-A) are used at each LED output to collimate it. A dichroic mirror (DM1: Thorlabs DMLP567L) with transmission band of 584-800 nm and cut-off wavelength of 567 nm, is used to pass the output of the red LED and reflects the output of the green one. Another dichroic mirror (DM2: Thorlabs DMLP490L) is used to pass the red and green LEDs outputs while reflects the output of the blue LED. The transmission band of this mirror is 505-800 nm with cut-off wavelength of 490 nm. Then the RGB single colour beams are transmitted over a distance of $d = 1$ m.

At the receiver side, the same configuration of the mirrors is used to separate the outputs of the three transmitters, where, another DM2: DM3 mirror is used to reflect the blue colour to its corresponding receiver while passes other two colours (red and green) through. Another DM1: DM4 mirror is used to pass the red LED towards its receiver while reflects the green colour towards the corresponding PD. Then another three aspheric condenser lenses (ACL4-6) are applied to focus the light of each LED into the detection area of its PD. The receivers (PDs) are selected to be PIN diode photodetector (PD: New Focus 1601 AC) with 3 dB bandwidth of 1 GHz which converts the incoming optical radiation into an electrical current signal. The PD has a built-in transimpedance amplifier (TIA) with gain of 10 V/mA that converts the current signal into a voltage signal. The received signals are then captured

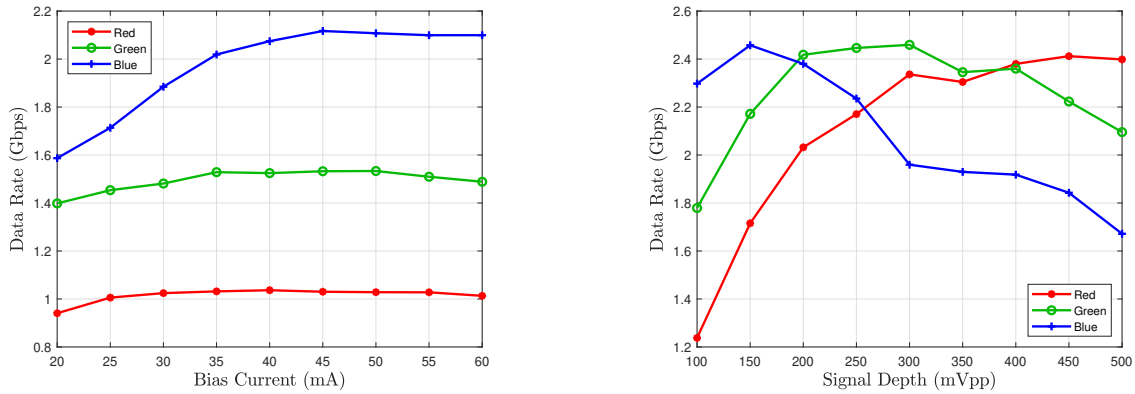

(a) (b)

Fig. 2: The system measured data rates for optimisation process. (a) data rate versus bias current (b) data rate versus signal depth

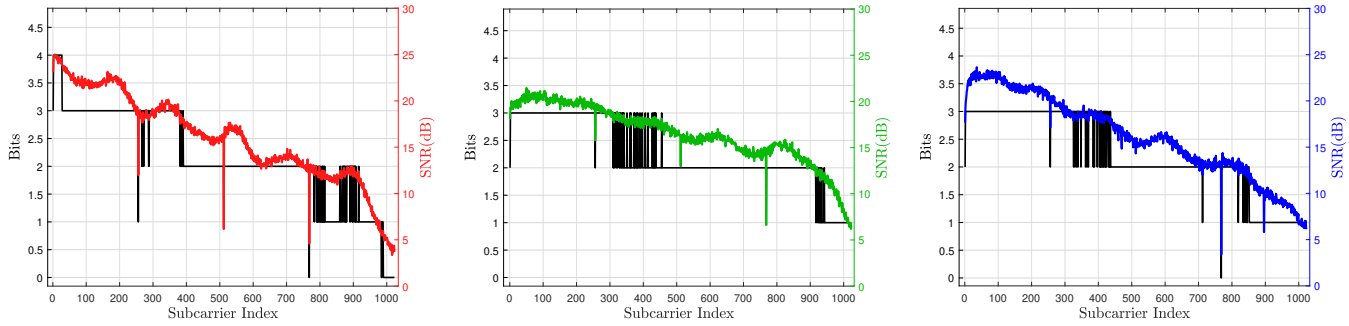

(a) Red LED (b) Green LED (c) Blue LED

Fig. 3: SNR and bits loaded per subcarrier for each LED

by a high speed oscilloscope (OSC: Keysight MSO-X 3104T) and then sent back to the laptop to be processed offline. Each received waveform is synchronised and down sampled then the CP is removed. This followed by fast Fourier transform (FFT) operation which provides the PAM signals in the frequency domain. The PA embedded pilots are extracted and their phase and amplitude are estimated using ML technique. The pilots estimated phases are used to restore the received data phase. The frequency domain signals are then equalised by their corresponding estimated channel frequency response followed by demodulation process using a PAM demodulator. The BER of each wavelength is evaluated from PAM demodulated symbols.

IV. Data Transmission Results and Discussions

As mentioned above, WDM using three single colour LEDs are used for PAM-DMT with PAPR reduction transmission. WDM is used with three LED colours RGB. The RGB single colour beams are combined at the transmitter (Tx) and separated at the receiver side (Rx) as shown in Fig. 1. The information is simultaneously transmitted and received over the three communication channels and the crosstalk between all channels is included in the system which makes it more close to practical applications. Moreover, the full modulation bandwidth of each RGB system is utilised with adaptive bit and power loading to maximise the spectral efficiency of each wavelength. In addition, The PAPR of PAM-DMT system of each LED is reduced by 10 iterations PA to minimise their nonlinearity effect and clipping distortion. Besides the above mentioned optimisation, system's parameters such as LED bias point and the peak-to-peak amplitude of each wavelength are optimised as well.

The system optimisation starts with the driving current point of each LED which determines the signal depth (Vpp) and nonlinearity effects. The experimental setup in section (III) is used for the optimisation process. The channel response and the available SNR at each subcarrier, SNR_k, per wavelength are estimated using multiple pilots composed of 4-QAM based optical OFDM frames. Error Vector Magnitude (EVM) method is used to evaluate the SNR_k of the received 4-QAM pilot frames [16]. The DC bias of each LED is found to minimise the LEDs nonlinearity and maximise the available SNR_k, and

consequently, increase the system achievable data rate.

For the optimisation, modulation bandwidth of 1 GHz per colour, number of active subcarriers N_{subs} of 1023 and IFFT size N of 2048 are used. The $N_{\mathrm{CP}} = 5$ is found to be sufficient for intersymbol interference (ISI) mitigation. First, the minimum possible V_{pp} of the AWG is selected which is found to be 75 mV, to avoid the nonlinearity effect of LEDs. Next, the bias current is increased gradually, and the system data rate is measured for each LED. It can be shown that, the maximum data rate for the green LED is found to be at 50 mA, while it is 45 mA for the red and blue LEDs as shown in Fig. 2a. The measured bias current points are used for finding the optimum signal depth V_{pp} points by increasing its value gradually and measuring the data rate for each colour. The optimum V_{pp} values are found to be 450 mV for the red LED, 300 mV for the green LED and 150 mV for the blue one as shown in Fig. 2b. The optimum bias current and signal depth values for each LED are used to measure the available SNR_k and the bit and power loaded per subcarrier k as shown in Fig. 3. This process results in achieving the highest possible data rates per wavelength.

Subsequently, the PA PAM-DMT data rate per wavelength is compared to that of conventional PAM-DMT without PAPR reduction. Note that both systems are using the same experimental setup and bit and power loading. The PA PAM-DMT data rate and BER results of each LEDs are tabulated in Table. I. The aggregate data rate for the PA PAM-DMT is 3.4885 Gb/s on the WDM system, where, the conventional PAM-DMT WDM system achieved 3.2339 Gb/s. This shows that, an increment of more than 8% when the high PAPR values are reduced by PA PAM-DMT.

Achieved Data Rate and BER				
Scheme	Metric	Red	Green	Blue
PAM-DMT	Rb (Gbps)	1.0774	1.0917	1.0648
	BER	0.0014	0.0010	0.0002
PA PAM-DMT	Rb (Gbps)	1.1689	1.1734	1.1462
	BER	0.0011	0.0008	0.0001

TABLE I: PA PAM-DMT and PAM-DMT performance comparison at optimum values

V. Conclusion

PA PAM-DMT based VLC is demonstrated experimentally using a WDM system employing three LEDs at different wavelengths. The system parameters such as bias current, I_{dc} and signal depth, V_{pp} are optimised and each LEDs' available modulation bandwidth is fully utilised with adaptive bit and power loading. The PAPR of PAM-DMT is reduced by 10 iterations PA scheme. PAPR reduction minimises the clipping noise and the nonlinearity distortion introduced by the light source. Reducing the PAPR of the PA PAM-DMT system results in more than 250 Mb/s data rate increase when compared to that of conventional PAM-DMT without PAPR reduction.

Acknowledgement

This research is funded in whole by Jazan University, Kingdom of Saudi Arabia. For the purpose of open access, the author has applied a Creative Commons Attribution (CC BY) licence to any Author Accepted Manuscript version arising from this submission.

References

[1] M. S. Islim, D. Tsonev, and H. Haas, "On the superposition modulation for OFDM-based optical wireless communication," in *2015 IEEE global conference on signal and information processing (GlobalSIP)*, pp. 1022–1026, IEEE, 2015.

[2] Z. Ghassemlooy, W. Popoola, and S. Rajbhandari, *Optical wireless communications: system and channel modelling with Matlab®*. CRC press, 2019.

[3] W. O. Popoola, Z. Ghassemlooy, and B. G. Stewart, "Pilot-Assisted PAPR Reduction Technique for Optical OFDM Communication Systems," *Journal of Lightwave Technology*, vol. 32, pp. 1374–1382, April 2014.

[4] J. Armstrong, "OFDM for Optical Communications," *Journal of Lightwave Technology*, vol. 27, pp. 189–204, Feb 2009.

[5] J. Armstrong, B. J. C. Schmidt, D. Kalra, H. A. Suraweera, and A. J. Lowery, "SPC07-4: Performance of Asymmetrically Clipped Optical OFDM in AWGN for an Intensity Modulated Direct Detection System," in *IEEE Globecom 2006*, pp. 1–5, 2006.

[6] S. C. J. Lee, S. Randel, F. Breyer, and A. M. J. Koonen, "PAM-DMT for Intensity-Modulated and Direct-Detection Optical Communication Systems," *IEEE Photonics Technology Letters*, vol. 21, pp. 1749–1751, Dec 2009.

[7] H. Alrakah, S. Sinanovic, and W. O. Popoola, "Pilot-Assisted PAPR Reduction in PAM-DMT based Visible Light Communication Systems," in *2021 IEEE Latin-American Conference on Communications (LATINCOM)*, pp. 1–6, 2021.

[8] M. S. Islim, D. Tsonev, and H. Haas, "Spectrally enhanced PAM-DMT for IM/DD optical wireless communications," in *2015 IEEE 26th Annual International Symposium on Personal, Indoor, and Mobile Radio Communications (PIMRC)*, pp. 877–882, 2015.

[9] W. O. Popoola, Z. Ghassemlooy, and B. G. Stewart, "Optimising OFDM based visible light communication for high throughput and reduced PAPR," in *2015 IEEE International Conference on Communication Workshop (ICCW)*, pp. 1322–1326, IEEE, 2015.

[10] Seung Hee Han and Jae Hong Lee, "An overview of peak-to-average power ratio reduction techniques for multicarrier transmission," *IEEE Wireless Communications*, vol. 12, pp. 56–65, April 2005.

[11] F. B. Offiong, S. Sinanović, and W. O. Popoola, "On PAPR Reduction in Pilot-Assisted Optical OFDM Communication Systems," *IEEE Access*, vol. 5, pp. 8916–8929, 2017.

[12] R. Bian, I. Tavakkolnia, and H. Haas, "15.73 Gb/s Visible Light Communication With Off-the-Shelf LEDs," *Journal of Lightwave Technology*, vol. 37, no. 10, pp. 2418–2424, 2019.

[13] H. Levin, "A complete and optimal data allocation method for practical discrete multitone systems," in *GLOBECOM'01. IEEE Global Telecommunications Conference (Cat. No.01CH37270)*.

[14] T. Z. Gutema and W. O. Popoola, "Single LED Gbps Visible Light Communication with Probabilistic Shaping," in *2021 IEEE Global Communications Conference (GLOBECOM)*, pp. 1–6, 2021.

[15] dialight, "Micro LED, Surface Mount LED Selector Guide," 2022. https://www.dialight.com/wp-content/uploads/2021/07/DIA_Selector_Guide_SMD_042321.pdf, Last accessed on 2022-02-25.

[16] R. A. Shafik, M. S. Rahman, and A. R. Islam, "On the Extended Relationships Among EVM, BER and SNR as Performance Metrics," in *2006 International Conference on Electrical and Computer Engineering*, pp. 408–411, 2006.